Published in final edited form as:

Hepatology. 2020 December ; 72(6): 2165–2181. doi:10.1002/hep.31239.

Impaired bile secretion promotes hepatobiliary injury in Sickle Cell Disease

Ravi Vats[1], **Silvia Liu**[2,7], **Junjie Zhu**[3], **Dhanunjay Mukhi**[4], **Egemen Tutuncuoglu**[1], **Nayra Cardenes**[1], **Sucha Singh**[2], **Tomasz Brzoska**[1], **Karis Kosar**[2], **Mikhil Bamne**[5], **Jude Jonassaint**[5], **Adeola Adebayo Michael**[2], **Simon C. Watkins**[4], **Cheryl Hillery**[5,6], **Xiaochao Ma**[3,7], **Kari Nejak-Bowen**[2,7], **Mauricio Rojas**[1,4], **Mark T Gladwin**[1,4,5,7], **Gregory J Kato**[1,4,5], **Sadeesh Ramakrishnan**[4,7], **Prithu Sundd**[1,4,5,7], **Satdarshan Pal Monga**[2,4,7,*], **Tirthadipa Pradhan-Sundd**[1,4,5,7,*]

[1]Pittsburgh Heart, Lung and Blood Vascular Medicine Institute, University of Pittsburgh School of Medicine, Pittsburgh, PA

[2]Dept. of Pathology, University of Pittsburgh School of Medicine, Pittsburgh, PA

[3]Center for Pharmacogenetics, Department of Pharmaceutical Sciences, School of Pharmacy, University of Pittsburgh, Pittsburgh, PA

[4]Department of Medicine, University of Pittsburgh School of Medicine, Pittsburgh, PA

[5]Sickle Cell Center for Excellence, University of Pittsburgh School of Medicine and University of Pittsburgh Medical Center, Pittsburgh, PA

[6]Department of Pediatrics, UPMC Children's Hospital of Pittsburgh, Pittsburgh, PA

[7]Pittsburgh Liver Research Center, University of Pittsburgh School of Medicine and University of Pittsburgh Medical Center, Pittsburgh, PA

Abstract

Hepatic crisis is an emergent complication affecting sickle cell disease (SCD) patients, however, the molecular mechanism of sickle cell hepatobiliary injury remains poorly understood. Using the knock-in humanized mouse model of SCD and SCD patient blood, we sought to mechanistically characterize SCD-associated hepato-pathophysiology applying our recently developed quantitative liver intravital imaging, RNA sequence analysis, and biochemical approaches. SCD mice manifested sinusoidal ischemia, progressive hepatomegaly, liver injury, hyperbilirubinemia, and increased ductular reaction under basal conditions. NF-κB activation in the liver of SCD mice

[*]To whom correspondence should be addressed: Tirthadipa Pradhan-Sundd, PhD, Research Assistant Professor, Department of Medicine, Division of Hematology-Oncology, University of Pittsburgh School of Medicine, E1225 BST, 200 Lothrop Street, Pittsburgh, PA, 15261, tip9@pitt.edu, Satdarshan P. S. Monga, MD, FAASLD, Endowed Chair for Experimental Pathology, Director: Pittsburgh Liver Research Center, Professor of Pathology (EP) & Medicine (Gastroenterology, Hepatology & Nutrition), University of Pittsburgh, School of Medicine, 200 Lothrop Street S-422 BST, Pittsburgh, PA 15261, Tel: (412) 648-9966; Fax: (412) 648-1916; smonga@pitt.edu.

Authors Contributions: Study concept and design: TP-S, SPM; acquisition of data: TP-S, RV, SS, DM, SK, JZ; analysis and interpretation of data: TP-S, SPM; drafting of the manuscript: TP-S, SPM, PS; critical revision of the manuscript for important intellectual content: TP-S, SPM, PS, SR, MG, XM, GK; statistical analysis: : NC,TP-S; obtained funding: TP-S, SPM, PS; technical, or material support: ET, TB, JZ, KK, MB, XM, SW, CH, K N-B, MR, GK, MG.

The authors have no conflict of interest to declare.

inhibited FXR signaling and its downstream targets, leading to loss of canallicular bile transport and altered bile acid pool. Intravital imaging revealed impaired bile secretion into the bile canaliculi, which was secondary to loss of canallicular bile transport and bile acid metabolism, leading to intrahepatic bile accumulation in SCD mice liver. Blocking NF-κB activation rescued FXR-signaling, and partially ameliorated liver injury and sinusoidal ischemia in SCD mice. These findings are the first to identify that NF-κB-FXR dependent impaired bile secretion promotes intrahepatic bile accumulation, which contributes to hepatobiliary injury of SCD. Improved understanding of these processes could potentially benefit the development of new therapies to treat sickle cell hepatic crisis.

INTRODUCTION

Sickle cell disease (SCD) is an autosomal-recessive monogenic disorder that affects approximately 100,000 Americans and millions of people worldwide[1]. Sickle Cell Anemia, the most common form of SCD is caused by a homozygous mutation in the β-globin gene leading to hemoglobin polymerization, erythrocyte rigidity, dehydration, vaso-occlusion (tissue-ischemia) and premature hemolysis[2,3]. Vaso-occlusion and hemolysis are the predominant pathophysiological events in SCD that contribute to multi-organ damage[4]. Although severely understudied, incidences of acute and chronic liver complications have increased over the last few decades due to the growing life expectancy of SCD patients. SCD associated liver complications are diverse[5] including cholestasis[6], choledocholethiasis[7], cholelithiasis and liver failure[8]. Hepatobiliary crisis is known to occur in up to 40% of hospitalized SCD patients but the molecular mechanism that promotes hepatobiliary injury in SCD is largely unknown[9]. Currently there are no standard diagnostic criteria or standardized therapeutic approaches for acute and chronic liver complications associated with SCD. Exchange blood transfusion which aims to reduce the sickling process has shown limited success in ameliorating all SCD associated liver symptoms. Thus, understanding of the pathophysiological mechanisms involved in this process is needed to identify new therapies for improved clinical outcomes.

Previous studies of liver disease in sickle cell patients were mostly based on autopsy and serum biochemical analyses[9,10]. Many of these studies have attributed hemolysis and vaso-occlusion as the primary regulators of hepatic dysfunction in SCD. However, studies aiming to understand the molecular mechanism of sickle hepatopathy are still lacking. We sought to mechanistically characterize SCD-associated hepato-pathophysiology using the well-characterized Townes knock-in humanized mouse model of SCD[11]. Using our recently developed quantitative liver intravital imaging (qLIM)[12], RNA sequence analysis (RNA-seq), and immunohistochemistry, we show for the first time that misexpression of bile transporters, intrahepatic bile accumulation, impaired bile secretion into the bile canaliculi and altered bile acid pool contribute to liver injury in SCD. Mechanistically, we demonstrate that sustained inflammation in SCD liver causes activation of NF-κB, which represses FXR signaling in SCD mice leading to impaired bile secretion and altered bile acid pool. In-depth molecular characterization of the role and regulation of NF-κB, FXR or bile acids modulations can be useful in identifying attractive therapeutic strategies for the management of the hepatic crisis in SCD.

METHODS

Human subjects

The human blood collection procedure has been described in detail elsewhere[13]. Blood samples were drawn from steady-state (not experiencing a vaso-occlusive pain episode) SCD or race-matched control healthy human subjects in sodium-citrate BD vacutainers at the Adult Sickle Cell Clinic of the University of Pittsburgh Medical Center. All participants gave written informed consent in accordance with the Declaration of Helsinki. Only nonsmokers who had not undergone an exchange transfusion within the last 60 days and who were diagnosed for SCD (SS) were included in the study. Additionally, only those SCD patients who were not experiencing an ongoing vaso-occlusive pain episode were included in the study and referred to as steady state patients. The demographic and clinical characteristics of the human subjects are shown in Supplemental Table 1 *and* 2.

Additional methods used in this study are standard and published, and are described in detail in the supplemental method section.

RESULTS

qLIM reveals ischemic liver injury in SCD mice

To characterize the liver injury in SCD mice, we used multi-photon-excitation (MPE) enabled *in vivo* real-time fluorescence microscopy of the intact liver in live mice (Figure 1A). The method of quantitative intravital liver imaging (*qLIM*) is described elsewhere[14]. Texas red (TXR)-dextran was intravascularly administered to visualize the blood flow in liver sinusoids of control and SCD mice. As shown in Figure.1B–B”, the blood flow (red) was normal within sinusoids of control mice (supplemental movies: 1, 2, 3). In contrast, SCD mice manifested complete loss of blood flow in several regions of the liver (Figure.1C–C”; supplemental movies: 4, 5, 6) at baseline. These regions appeared black due to the absence of TXR-dextran, suggestive of sinusoidal ischemia. When measured, around 40% of the liver sinusoids in SCD mice had a loss of blood flow compared to almost none in control mice (Figure. 1D). The average number of vaso-occlusion per field of view was as high as 0.8 (Figure 1E).

To identify the pathways associated with ischemic injury in SCD mice liver, we performed RNA-seq analysis using the liver of SCD and control mice at baseline. Pairwise analyses between control and SCD mice liver identified mRNA expression of a total of 24,419 genes. A comparison of the total number of differentially expressed genes in each pairwise analysis (FDR<0.01; Fold change≥5) revealed a change in expression of 265 genes (Figure S1A). Interestingly, the maximum fold change in SCD mice liver was associated with genes related to fibrosis (MMPs and collagens, GGTs) (Figure S1B), inflammation associated genes (CCL4, CCL6, CD24 and 36) (Figure S1C,E) and P53 signalling pathway (Figure S1D). Interestingly, genes involved in bile acid metabolism (Figure S1F) and fatty acid metabolism (Figure S1F) also showed significant misexpression in the liver of SCD mice. Finally, as expected in SCD[15,16], we also found significant fold changes in genes related to hemoglobin metabolism, regulators of erythropoiesis and pathways involved in hemoglobin synthesis and regulation (Figure S2A–D).

Ischemia-reperfusion is known to contribute to progressive liver injury[17] and our RNA seq study showed upregulation of genes involved in fibrosis and inflammation (Figure S1B–E). Therefore, we next analyzed the gross liver injury in SCD mice. The liver of 12–15 week old SCD mice was larger (Figure.2A) and stiffer, with a greater liver to body weight ratio (LW/BW) than control mice, and manifested white spots indicative of ischemic tissue damage (Figure.2A). Blood serum analysis showed a comparable amount of triglyceride, glucose, cholesterol, albumin and gGTP levels (Figure.S4D) in SCD and control mice. However, a significant increase in serum alanine aminotransferase (ALT) and aspartate transaminase (AST) was observed in SCD mice, indicative of progressive liver injury (Figure. 2A). In contrast, alkaline phosphatase (ALP), a marker of ductular injury appeared comparable in control and SCD mice (Figure. 2A). SCD mice also exhibited high levels of total and direct serum bilirubin (Figure 2A). Taken together, our data suggest that SCD mice develop liver injury under baseline conditions, which is associated with sinusoidal ischemia, tissue damage, hyperbilirubinemia and elevated levels of liver enzymes.

SCD mice manifest liver fibrosis, cell death and increased ductular reaction.

Next, we performed histology and IHC for injury and inflammation markers in the liver of SCD mice. Steatohepatitis and increased injury were evident by H&E in SCD mice livers (Figure 2B, S3). Sirius red (Figure 2B,C, S3) and α-SMA (Figure 2B,C, S3) staining showed extensive collagen deposition and activated myofibroblasts in SCD mice liver, respectively suggestive of liver fibrosis. TUNEL staining, which labels apoptotic cells were increased in the livers of SCD mice as compared to control mice (Figure 2B,D). Oil red O staining showed prominent lipid accumulation in SCD liver (Figure 2B,E). Next we examined the hydroxyproline content in control and SCD liver tissue to analyze the extent of liver fibrosis. As shown in Figure 2F, SCD liver showed a significant increase in hydroxyproline content compared to control. Intrahepatic cholestasis is believed to be one of the causes of liver failure in SCD patients[10,18]. IHC analysis based on staining for cholangiocyte markers CK-19 (Figure 3A–B), EpCAM (Figure 3C–D) and Sox-9 (Figure 3E–F) showed a notable ductular response in the livers of SCD mice compared to controls. These changes were more pronounced in larger ductal areas of the livers, which had extensive portal tracts containing reactive ductules and inflammatory cells (Figure 3A–F, S4B). Furthermore, RT-PCR analysis of the whole livers also showed a significant increase in the mRNA levels of CK-19 (Figure S4A), EpCAM (Figure S4A) and Sox-9 (Figure S4A) in SCD compared to control mice livers. Although the larger ducts (large mouse cholangiocytes; LMCCs) showed increased expression of ductular markers (Figure S4B), the smaller ducts of SCD mice liver (small mouse cholangiocytes; SMCCs) showed weaker or almost complete loss of Ck-19/EpCAM staining (Figure S4B). It has been proposed that SMCCs contain a population of biliary progenitor cells and express various biliary progenitor markers[19]. We performed RT-PCR for markers known to be enriched in SMCC. Intriguingly, we found significant reduction in FoxA2 and Sox-17 (Figure S4C) indicating a potential defect in SMCC development. Collectively, our data suggest that SCD mice showed liver fibrosis, steatohepatitis, inflammation and cholestasis.

qLIM reveals delayed bile transport in SCD mice

To further validate the presence of cholestasis in SCD mice, we used qLIM to assess real time bile and blood flow in the liver of SCD mice. IV administration of Texas-Red (TXR)-dextran (red) was used to visualize the blood flow through liver sinusoids and carboxyfluorescein (CF; green) to visualize bile flow through biliary canaliculi[14] of the intact liver in live mice (Figure 4A). As previously described[14], the uptake of CF in hepatocytes of control mice occurred within 1 min after injection (Figure.4Bb–b',supplemental movie: 7), and CF appeared as linear green pattern outlining the hepatocytes (Figure.4Bb–b' supplemental movie: 7). The sinusoidal vessels containing TXR-dextran were visible as red fluorescence (Figure.4Bb–b'). At 3–4 min, CF was localized prominently to biliary canaliculi (Figure.4Bc–c' supplemental movie: 8). By 5 min, CF was exclusively present in bile canaliculi (Figure.4Bd–d', supplemental movie: 9) and no CF localization was observed in hepatocytes after this time point. Unlike control mice, CF failed to completely exit the hepatocytes within 3–5 minutes of IV administration in SCD mice (Figure.4Be–e' supplemental movies: 10, 11) and CF localization was present in hepatocytes even after 10 minutes (Figure.4Bf–f', g–g', supplemental movie: 12) suggesting a delayed bile transport in SCD mice. When measured, CF staining showed significant enrichment in hepatocytes at any given time points in the liver of SCD mice (Figure 4C).

Impaired bile secretion in SCD is associated with increased cholangiocyte senescence

We evaluated the markers of inflammation to address the potential role of inflammation in promoting impaired bile secretion[20,21] in SCD mice. An increase in F4/80 (Figure 5A) as well as CD45 staining (Figure 5A) compared to control liver indicated a periductal and parenchymal inflammatory response in the liver of SCD mice. Expression (mRNA levels) of pro-inflammatory cytokines TNFα, IL-1β and IL-6 were also significantly upregulated (Figure 5B) in SCD mice compared to control mice. Abnormally proliferating cholangiocytes can become senescent and produce pro-inflammatory factors that contribute to the pathogenesis of cholestasis[22]. We assessed p21, a marker and mediator of cellular senescence[23] by IHC and found increased number of p21-positive cholangiocytes (Figure 5C) in SCD mice liver compared to none in littermate control mice liver (Figure 5C). Co-localization of P21 with cholangiocyte marker CK19 further confirmed this (Figure 5C) in SCD liver. RT-PCR (Figure 5C) and western blot (Figure 5C) analysis also showed a significant upregulation of p21 expression in SCD livers compared to control. Interestingly, another regulator of cellular senescence, $p16^{INK4a}$ also showed a significant upregulation (Figure 5C) by RT-PCR compared to control. Thus inflammation, increased ductular response and impaired bile secretion in SCD mice liver is associated to cholangiocyte senescence.

NF-κB and its downstream targets are upregulated in SCD liver

Given that SCD mice show a significant increase in P21 levels in cholangiocytes, we hypothesized the potential activation of the nuclear factor kappa B (NF-κB) pathway in the liver of SCD mice[24,25]. An evaluation of NF-κB and target genes by RNA seq (Figure 5D) revealed generalized activation in SCD mice liver. Further validation using qRT-PCR confirmed significant upregulation of the mRNA expression of NF-κB1, NF-κB2, v-rel

avian reticuloendotheliosis viral oncogene homolog A (RelA), v-rel avian reticuloendotheliosis viral oncogene homolog B (RelB), intercellular adhesion molecule 1 (ICAM1) and vascular cell adhesion molecule 1 (VCAM1) in the liver of SCD mice compared to control mice (Figure 5D'). Moreover, NF-κB (P65) protein expression was found significantly enriched in the cholangiocytes and hepatocytes of SCD mice (Figure 5E), by IHC, which was absent in littermate controls (Figure 5E). This was further validated with western blot using antibodies against phospho-P65, which showed a significant upregulation (Figure 5F) in the liver of SCD mice compared to control liver. NF-κB activation was further substantiated by the increase of NF-κB(p65) and downstream targets Traf-1 and Fas (Figure 5F). Thus, these data suggest that NF-κB and its downstream targets are upregulated in SCD liver.

Activated NF-κB suppresses FXR signaling in SCD liver

Inflammation induced activation of NF-κB has been shown to downregulate farnesoid X receptor (FXR) and its target genes in models of inflammation induced and obstructive cholestasis[26,27]. We hypothesized that activation of NF-κB in the liver of SCD mice leads to the downregulation of FXR and its targets which in turn promotes impaired bile secretion. Interestingly, the m-RNA expression of FXR showed a moderate reduction (Figure. 6A) in the liver of SCD mice compared to control mice by qRT-PCR. FXR induces the expression of small heterodimer partner (SHP). Remarkably, SHP mRNA expression was significantly downregulated (Figure 6A) in SCD compared to the control mice liver. Moreover, qRT-PCR analysis showed a significant reduction of apical (canalicular) bile acid transporters BSEP, ABCG5 and ABCG8 and MRP2 (Figure. 6A), in SCD mice liver which are known FXR targets[28,29]. An evaluation of FXR target genes by RNA-seq further confirmed a generalized suppression in SCD liver (Figure 6C).

Loss of canalicular transporters could possibly lead to impaired bile flow to the canaliculi, which in turn may lead to intrahepatocyte accumulation of bile as shown in Figure 4B. Therefore, we next looked at efflux transporters that can promote reentry of bile acids from hepatocytes to liver sinusoids. Remarkably, the efflux transporters MRP1,4, and 5 were several fold upregulated (Figure 6A) in the SCD mice liver indicating that intrahepatic bile accumulation in SCD is also associated with subsequent reflow of bile from hepatocytes into the sinusoidal blood. Interestingly, no significant changes were observed in basolateral transporters OATP-1 and OATP-2 (Figure 6A). As a net result of these alterations in bile acids transport, total bile acids levels in the liver (Figure 6B) were increased in SCD mice.

In addition to its inhibitory effects on the expression of FXR target genes, NF-κB has also been shown to physically associate with FXR in the liver[30]. We next analyzed if there is an increased physical interaction between NF-κB and FXR in SCD liver through immunoprecipitation (IP) studies using whole-cell lysates from control and SCD livers. IP of lysates with FXR antibody demonstrated an association of FXR with NF-κB in control livers at baseline (Figure 6D); notably, this interaction was mildly increased in SCD livers (Figure 6D). Next, we sought to determine if there was any evidence of competitive antagonism between NF-κB and RXRα (FXR binding partner) for FXR. Remarkably, compared to control, the association of FXR with RXR was reduced in SCD liver (Figure 6E).

Conversely, we found a physical association between NF-κB and RXR in the control liver and this interaction was significantly increased in SCD livers (Figure 6E). Thus, NF-κB levels inversely correlated with FXR target gene activation in SCD, with excess NF-κB competing and sequestering FXR binding to RXR, resulting in suppression of downstream signaling. We conclude that FXR pathway inhibition alters bile transporter levels leading to impaired bile secretion and increased hepatobiliary injury associated with SCD.

Sustained inflammation alters hepatic bile acid pool in SCD

NF-κB driven chronic inflammation has been previously shown to regulate cholesterol and bile acid metabolism[31]. Similarly, altered FXR signaling is known to cause impaired bile acid metabolism[32]. As we see increased hepatic bile acids in SCD mice along with NF-κB driven loss of FXR pathway targets, we next analyzed the total cholesterol level in SCD mice. Whereas serum cholesterol levels were comparable (Figure S4D), the hepatic total cholesterol levels were mildly upregulated (Figure S4E) in SCD compared to control mice, indicating aberrant cholesterol metabolism and accumulation of cholesterol and bile acid precursors, leading to toxicity in the liver of SCD mice. To confirm altered the bile acid pool in SCD, we performed detailed analysis of bile acid composition in the liver of control and SCD mice. Remarkably, tauro-β-muricholic acid (TβMCA), which is known to cause increased bile acid toxicity and intrahepatic cholestasis[33,34], was significantly upregulated in the liver of SCD mice (Figure 6F). This resulted in a dramatic alteration of the bile acid pool in the SCD liver, from predominantly taurocholic acid (TCA) in the control liver (Figure 6F,) to predominantly TβMCA in SCD liver (Figure 6F). Thus we conclude that NF-κB driven loss of FXR signaling not only increases total hepatic bile acid levels leading to hepatobiliary injury, but also alters bile acid composition to a more toxic bile acid pool promoting further injury.

Finally, to validate our findings in SCD mouse model, we analysed SCD patient's (at steady-state, without notable crisis and without a history of a recent blood transfusions) serum samples. Identical to previous findings in SCD patients[35], serum ALP was upregulated in SCD patients (Figure S5A). Interestingly, total and direct bilirubin levels also showed a significant increase in SCD patients compared to control human subjects (Figure S5B). Whereas serum cholesterol levels appeared comparable, serum triglyceride levels were found to be reduced in these SCD patients (Figure S5C). Since SCD mice manifested impaired bile secretion and altered bile acid pool (Figure 6B), we next analyzed serum bile acid levels in SCD and control human subjects. Remarkably, total serum bile acid levels were increased in all SCD compared to control human subjects (Figure S5D). Moreover, analysis of bile acid composition in the serum of SCD human subjects revealed similar defects as found in SCD mice (Figure S5E,F). We found a significant increase in glycine (predominantly present in humans instead of taurine) conjugated secondary bile acids glycocholic acid (GCA), glycodeoxycholic acid (GDCA), and glycochenodeoxycholic acid (GCDCA) in SCD patients (Figure S5EF). Altered expression of GDCA and GCDCA have been linked with liver fibrosis, acute injury and liver failure[36,37]. Altogether, these findings indicate a drastic change in bile acid composition resulting in an increase in bile toxicity in the liver of SCD mice and SCD patient serum sample.

N-Acetyl-L-(+)-cysteine (NAC) can partially ameliorate liver injury in SCD mice

Since we found activation of NF-κB in SCD liver, we hypothesized that blocking NF-κB pathway might ameliorate the liver injury phenotypes associated with SCD. We administered N-Acetyl-L-(+)-cysteine (NAC) which has been used extensively as a NF-κB suppressor[38–41] to control and SCD mice via drinking water for upto 12 weeks (Figure 7A). NAC administration was able to reduce the protein expression of NF-κB(P65) as seen by western blot (Figure 7B). Moreover, qRT-PCR assay showed reduced mRNA expression of NF-κB and its target genes including ICAM-1, VCAM-1 and iNOS in the liver of SCD mice (Figure 7B). NAC treatment also led to a decrease in liver injury seen by reduced level of ALT and direct bilirubin whereas AST and total bilirubin level were unchanged (Figure 7C). H&E, Sirius red and α-SMA staining showed a decrease in sinusoidal congestion, injury and fibrosis (Figure.7D) in SCD mice liver after NAC treatment.

Next, we used qLIM imaging in live mice. As shown in Figure7E, SCD mice manifested complete loss of blood flow in several regions of the liver (Figure1C,7E; supplemental movies: 4, 5, 6) at baseline due to sinusoidal vaso-occlusion. Remarkably, SCD mice on NAC treatment showed attenuation of vaso-occlusion. Only a few small areas with loss of blood flow were observed in SCD mice with NAC treatment compared to large vaso-occlusion seen in the liver of untreated SCD mice (Figure 7E). When quantified, SCD mice on NAC treatment showed a significant reduction in liver sinusoidal vaso-occlusion (Figure 7E). Finally, we examined the mRNA expression of FXR and its target genes by qRT-PCR in SCD mice with and without NAC treatment. Remarkably, the liver of NAC-treated SCD mice showed reappearence of FXR and its target genesincluding Shp1, ABCG8, MRP2 (Figure 7F). Thus, blocking NF-κB pathway partially prevented hepato-biliary manifestations and rescued FXR-signaling in the SCD mouse liver.

DISCUSSION

SCD affects millions of people world-wide with an estimated annual medical cost over $1.1 billion in the US[42]. Clinical evidence suggests that the incidence of hepatobiliary injury is associated with increased mortality among SCD patients[43]. We show for the first time that NF-κB activation in SCD mice liver suppresses FXR signaling, which promotes intrahepatic accumulation of cholesterol and bile acids, delayed bile secretion into the bile canaliculi and altered bile acid pool (Figure 8). Blocking NF-κB led to partial amelioration of the liver injury in SCD mice.

We found sinusoidal ischemia in the liver of SCD mice under baseline conditions, which was associated with progressive hepatomegaly, liver fibrosis, ductular reaction and upregulated mRNA levels of various inflammatory markers suggestive of chronic inflammation. Mechanistically, we demonstrate that sustained inflammation in SCD liver causes activation of NF-κB and its target genes which repressed FXR signaling in the liver of SCD mice, leading to misexpression of canalicular bile transporters, intrahepatic bile accumulation, and altered bile acid composition.

Activated NF-κB competitively inhibited RXR binding to FXR in SCD mice liver, which led to the suppression of FXR target genes BSEP, ABCG5, ABCG8 and MRP2. FXR

contributes to the homeostasis of liver metabolism including bile synthesis, transport, detoxification and excretion[32,44,45]. The loss of FXR signaling has been shown to promote bile toxicity induced hepatic injury and mice genetically deficient in FXR manifest severe liver inflammation and bile toxicity[46]. Indeed, toxic hydrophobic bile acids such as TβMCA in SCD mice and GDCA, and GCDCA in SCD patients were significantly upregulated compared to control mice and humans, respectively. Taken together, the current and previous findings suggest that the loss of FXR signaling may contribute to hepatobiliary injury in SCD mice. These findings also suggest that agonists of FXR signaling can be therapeutically useful to attenuate hepatobiliary injury in SCD, and serum bile acid analysis can be a potential biomarker to identify SCD patients at risk of developing hepatic crisis.

Blocking NF-κB attenuated vasoocclusion, partially ameliorated liver injury and reduced both ALT and direct bilirubin levels. Remarkably, we also saw reappearance of FXR and some of its target genes in the liver of SCD mice upon NF-κB activation. Taken together, these findings suggest that NF-κB activation contributes to vasoocclusion and liver injury in SCD.

Our findings are associated with few limitations that warrant further investigation in future studies. First, although elevated ALP levels are considered as a biomarker for cholestasis, SCD mice manifested significant increase in the ductular reaction without an increase in ALP levels. In contrast, ALP was increased at baseline in SCD patients. We believe that disease heterogeneity[48] and comorbidities often observed in SCD patients contributes to this discrepancy. Second, the current study is the first to establish that loss of canalicular bile transporters are associated with hepatobiliary injury of SCD, however, the cause and effect relationship between these pathological events remains to be elucidated. Third, we see significant upregulation of NFkB and its target genes. We also see a significant increase in TNFα, which is a known inducer of NFkB pathway. However, it remains to be investigated whether NFkB activation in SCD liver is TNFα dependent or it is a consequence of the intrahepatic accumulation of toxic bile secondary to loss of bile transporters. Similarly, blocking NF-κB using NAC only partially ameliorated SCD associated liver injury, suggesting that additional factors also contribute to hepatobiliary injury of SCD. Fourth, our study shows an increase in taurine (mice) and glycine (human) conjugated secondary bile acids in SCD, which has been previously shown to be associated with prolonged exposure to antibiotics resulting in loss of gut microbiota[49]. Interestingly, aberrant gut microbiome was recently shown to promote inflammation and systemic ischemia in SCD mice[50]. Thus future investigations should explore the role of microbiome and altered composition of bile acids in promoting hepatobiliary injury in SCD. Notwithstanding these limitations, the current study is the first to identify that impairment of bile acid secretion in hepatocytes is associated with the development of sickle cell hepatobiliary injury. Improved understanding of these processes could potentially benefit the development of new therapies and biomarkers to treat or prevent sickle cell hepatic crisis.

Supplementary Material

Refer to Web version on PubMed Central for supplementary material.

Acknowledgments

Financial Support: This work was supported by Pittsburgh Liver Research Centre Pilot grant, Community Liver Alliance Pilot Grant and NIH-NIDDK 5T32DK639-22 (13) to TP-S; NIH-NIDDK (DK62277, DK100287, and CA204586) to S.P.M.. S.P.M is the Endowed Chair for Experimental Pathology, University of Pittsburgh School of Medicine. NIH-NHLBI 1R01HL128297-01, 1R01HL141080-01A1, American Heart Association 18TPA34170588 and funds from the Hemophilia Center of Western Pennsylvania and Vitalant to PS. RV was supported by American Heart Association 19PRE34430188. The Nikon multiphoton excitation microscope was funded by NIH grant 1S10RR028478-01 (SCW).

Bibliography

1. Ware RE, de Montalembert M, Tshilolo L & Abboud MR Sickle cell disease. The Lancet 390, 311–323 (2017).
2. Sundd P, Gladwin MT & Novelli EM Pathophysiology of Sickle Cell Disease - Elsevier Medical Artwork. Annual Review ofPathology (2018). doi:10.1146/annurevpathmechdis-012418-012838
3. Frenette PS & Atweh GF Sickle cell disease: old discoveries, new concepts, and future promise. The Journal of Clinical Investigation 117, 850–858 (2007). [PubMed: 17404610]
4. Powars DR Sickle cell anemia and major organ failure. Hemoglobin 14, 573–98 (1990). [PubMed: 2101835]
5. Baichi MM, Arifuddin RM, Mantry PS, Bozorgzadeh A & Ryan C Liver transplantation in sickle cell anemia: a case of acute sickle cell intrahepatic cholestasis and a case of sclerosing cholangitis. Transplantation 80, 1630–2 (2005). [PubMed: 16371935]
6. KLION FM, WEINER MJ & SCHAFFNER F CHOLESTASIS IN SICKLE CELL ANEMIA. The American journal of medicine 37, 829–32 (1964). [PubMed: 14237437]
7. Mills LR, Mwakyusa D & Milner PF Histopathologic features of liver biopsy specimens in sickle cell disease. Archives of pathology & laboratory medicine 112, 290–4 (1988). [PubMed: 3345126]
8. Hurtova M et al. Transplantation for liver failure in patients with sickle cell disease: Challenging but feasible. Liver Transplantation 17, 381–392 (2011). [PubMed: 21445921]
9. Schubert TT Hepatobiliary system in sickle cell disease. Gastroenterology 90, 2013–21 (1986). [PubMed: 3516788]
10. Shao SH & Orringer EP Sickle cell intrahepatic cholestasis: approach to a difficult problem. The American journal of gastroenterology 90, 2048–50 (1995). [PubMed: 7485022]
11. Wu LC et al. Correction of sickle cell disease by homologous recombination in embryonic stem cells. Blood 108, 1183–1188 (2006). [PubMed: 16638928]
12. Pradhan-Sundd T et al. Dual catenin loss in murine liver causes tight junctional deregulation and progressive intrahepatic cholestasis. Hepatology 67, (2018).
13. Bennewitz MF et al. Lung vaso-occlusion in sickle cell disease mediated by arteriolar neutrophil-platelet microemboli. JCI Insight 2, (2017).
14. Pradhan-Sundd T et al. Dysregulated bile transporters and impaired tight junctions during chronic liver injury in mice. Gastroenterology (2018). doi:10.1053/j.gastro.2018.06.048
15. Ferreira A et al. Sickle hemoglobin confers tolerance to plasmodium infection. Cell (2011). doi:10.1016/j.cell.2011.03.049
16. Akinsheye I et al. Fetal hemoglobin in sickle cell anemia. Blood (2011). doi:10.1182/blood-2011-03-325258
17. Tsung A et al. The nuclear factor HMGB1 mediates hepatic injury after murine liver ischemia-reperfusion. The Journal of Experimental Medicine (2005). doi:10.1084/jem.20042614
18. Guimarães J. A. de & Silva LC dos S. Sickle cell intrahepatic cholestasis unresponsive to exchange blood transfusion: a case report. Revista Brasileira de Hematologia e Hemoterapia 39, 163–166 (2017). [PubMed: 28577654]
19. Alpini G et al. Morphological, molecular, and functional heterogeneity of cholangiocytes from normal rat liver. Gastroenterology (1996). doi:10.1053/gast.1996.v110.pm8613073
20. Dominical VM et al. Interactions of sickle red blood cells with neutrophils are stabilized on endothelial cell layers. Blood Cells, Molecules, and Diseases 56, 38–40 (2016).

21. Trauner M, Fickert P & Stauber RE Inflammation-induced cholestasis. Journal of Gastroenterology and Hepatology (Australia) (1999). doi:10.1046/j.1440-1746.1999.01982.x
22. O'Brien A et al. The Role of Cholangiocyte Cell Death in the Development of Biliary Diseases. in Molecules, Systems and Signaling in Liver Injury (2017). doi:10.1007/978-3-319-58106-4_2
23. Passos JF et al. Feedback between p21 and reactive oxygen production is necessary for cell senescence. Molecular Systems Biology (2010). doi:10.1038/msb.2010.5
24. Rovillain E et al. Activation of nuclear factor-kappa B signalling promotes cellular senescence. Oncogene (2011). doi:10.1038/onc.2010.611
25. Luedde T & Schwabe RF NF-κB in the liver-linking injury, fibrosis and hepatocellular carcinoma. Nature Reviews Gastroenterology and Hepatology (2011). doi:10.1038/nrgastro.2010.213
26. Huang W, Wang YD & Chen WD FXR, a target for different diseases. Histology and Histopathology 23, 621–627 (2008). [PubMed: 18283647]
27. Vavassori P, Mencarelli A, Renga B, Distrutti E & Fiorucci S The Bile Acid Receptor FXR Is a Modulator of Intestinal Innate Immunity. The Journal of Immunology (2009). doi:10.4049/jimmunol.0803978
28. Ananthanarayanan M, Balasubramanian N, Makishima M, Mangelsdorf DJ & Suchy FJ Human Bile Salt Export Pump Promoter Is Transactivated by the Farnesoid X Receptor/Bile Acid Receptor. Journal of Biological Chemistry (2001). doi:10.1074/jbc.M011610200
29. Yu L et al. Expression of ABCG5 and ABCG8 is required for regulation of biliary cholesterol secretion. Journal of Biological Chemistry (2005). doi:10.1074/jbc.M411080200
30. Balasubramaniyan N, Ananthanarayanan M & Suchy FJ Nuclear factor-κB regulates the expression of multiple genes encoding liver transport proteins. American Journal of Physiology-Gastrointestinal and Liver Physiology (2016). doi:10.1152/ajpgi.00363.2015
31. He M et al. Pro-inflammation NF-κB signaling triggers a positive feedback via enhancing cholesterol accumulation in liver cancer cells. Journal of Experimental and Clinical Cancer Research (2017). doi:10.1186/s13046-017-0490-8
32. Eloranta JJ & Kullak-Ublick GA The Role of FXR in Disorders of Bile Acid Homeostasis. Physiology 23, 286–295 (2008). [PubMed: 18927204]
33. Li F et al. Microbiome remodelling leads to inhibition of intestinal farnesoid X receptor signalling and decreased obesity. Nature Communications (2013). doi:10.1038/ncomms3384
34. Degirolamo C, Rainaldi S, Bovenga F, Murzilli S & Moschetta A Microbiota modification with probiotics induces hepatic bile acid synthesis via downregulation of the Fxr-Fgf15 axis in mice. Cell Reports (2014). doi:10.1016/j.celrep.2014.02.032
35. Zorca S et al. Lipid levels in sickle-cell disease associated with haemolytic severity, vascular dysfunction and pulmonary hypertension. British Journal of Haematology (2010). doi:10.1111/j.1365-2141.2010.08109.x
36. Woolbright BL et al. Glycodeoxycholic acid levels as prognostic biomarker in acetaminophen-induced acute liver failure patients. Toxicological Sciences (2014). doi:10.1093/toxsci/kfu195
37. Chen T et al. Serum and urine metabolite profiling reveals potential biomarkers of human hepatocellular carcinoma. Molecular and Cellular Proteomics (2011). doi:10.1074/mcp.M110.004945
38. Oka SI, Kamata H, Kamata K, Yagisawa H & Hirata H N-Acetylcysteine suppresses TNF-induced NF-κB activation through inhibition of IκB kinases. FEBS Letters (2000). doi:10.1016/S0014-5793(00)01464-2
39. Blackwell TS, Blackwell TR, Holden EP, Christman BW & Christman JW In vivo antioxidant treatment suppresses nuclear factor-kappa B activation and neutrophilic lung inflammation. Journal of immunology (Baltimore, Md. : 1950) (1996).
40. Finn NA & Kemp ML Pro-oxidant and antioxidant effects of N-acetylcysteine regulate doxorubicin-induced NF-kappa B activity in leukemic cells. Molecular BioSystems (2012). doi:10.1039/c1mb05315a
41. Kretzmann NA, Chiela E, Matte U, Marroni N & Marroni CA N-acetylcysteine improves antitumoural response of Interferon alpha by NF-kB downregulation in liver cancer cells. Comparative Hepatology (2012). doi:10.1186/1476-5926-11-4

42. Hassell KL Population Estimates of Sickle Cell Disease in the U.S. American Journal of Preventive Medicine 38, S512–S521 (2010). [PubMed: 20331952]
43. Galloway-Blake K, Reid M, Walters C, Jaggon J & Lee MG Clinical Factors Associated with Morbidity and Mortality in Patients Admitted with Sickle Cell Disease. West Indian Med J 63, 711–716 (2014). [PubMed: 25867578]
44. Wagner M et al. Role of Farnesoid X Receptor in Determining Hepatic ABC Transporter Expression and Liver Injury in Bile Duct–Ligated Mice. doi:10.1016/S0016-5085(03)01068-0
45. Chiang JYL Bile acids: regulation of synthesis. Journal of Lipid Research (2009). doi:10.1194/jlr.R900010-JLR200
46. Kong B et al. Mechanism of tissue-specific farnesoid X receptor in suppressing the expression of genes in bile-acid synthesis in mice. Hepatology (2012). doi:10.1002/hep.25740
47. Koseoglu M, Hur A, Atay A & Çuhadar S Effects of hemolysis interferences on routine biochemistry parameters. Biochemia Medica (2011). doi:10.11613/bm.2011.015
48. Schaefer BA et al. Genetic modifiers of white blood cell count, albuminuria and glomerular filtration rate in children with sickle cell anemia. PLoS ONE 11, 1–14 (2016).
49. Sayin SI et al. Gut microbiota regulates bile acid metabolism by reducing the levels of tauro-beta-muricholic acid, a naturally occurring FXR antagonist. Cell Metabolism (2013). doi:10.1016/j.cmet.2013.01.003
50. Zhang D et al. Neutrophil ageing is regulated by the microbiome. Nature (2015). doi:10.1038/nature15367

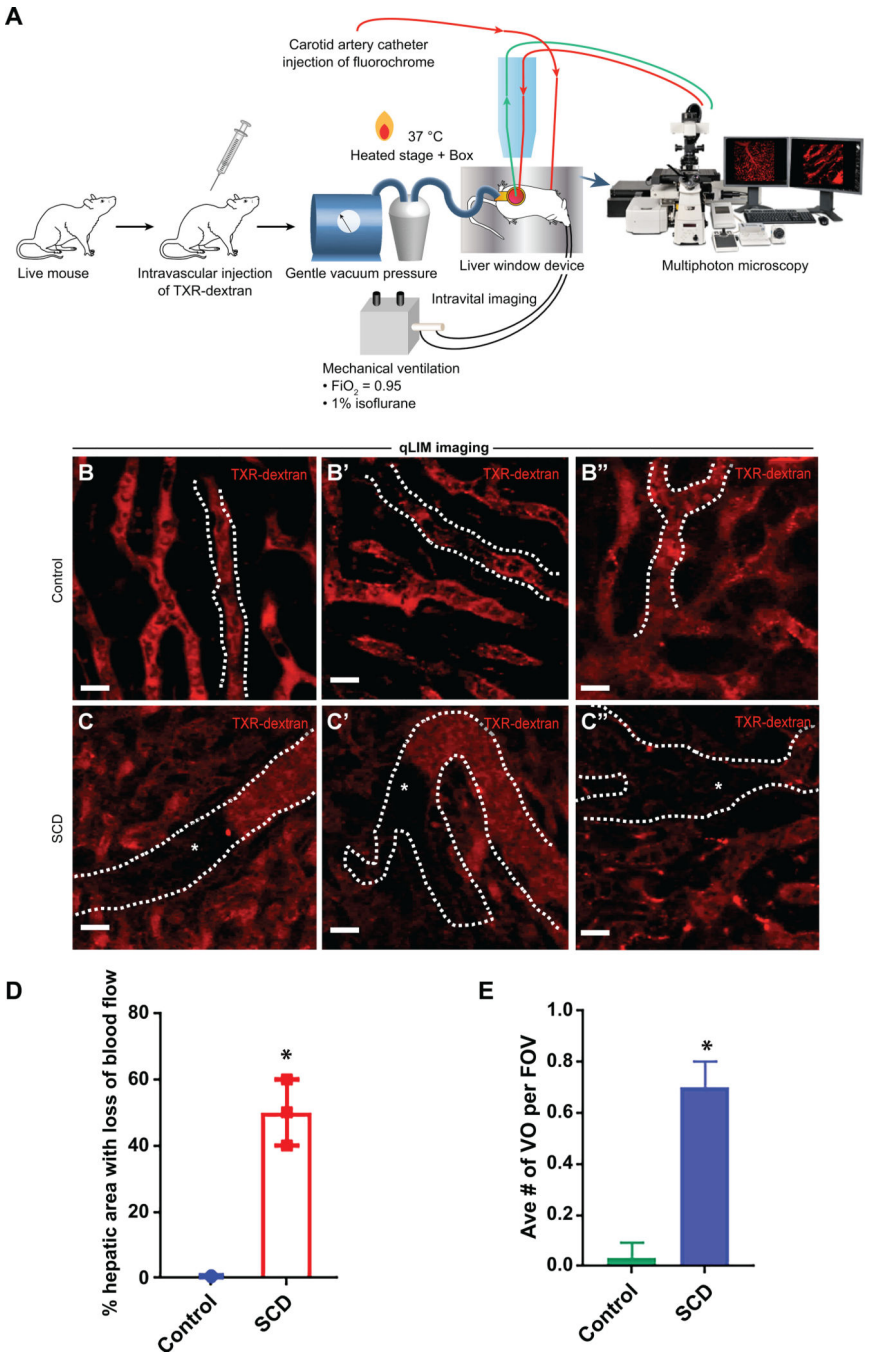

Figure 1: SCD mice exhibit ischemic liver injury at baseline.

(A) Schematic diagram of quantitative liver intravital (qLIM) imaging of mice using TXR-dextran. qLIM images of three different fields of view of **(B-B")** control and (**C-C"**) SCD liver injected with TXR-dextran. Arrow indicates the flow of blood across the liver sinusoids. Dotted line marks the sinusoids. * shows loss of blood flow in SCD liver. **(D)** Quantification of the total area (%) of liver with loss of blood flow and **(E)** average number of vassocclusion per field of view in SCD and control mice.. * denotes $p<0.05$. Scale bar 30 um.

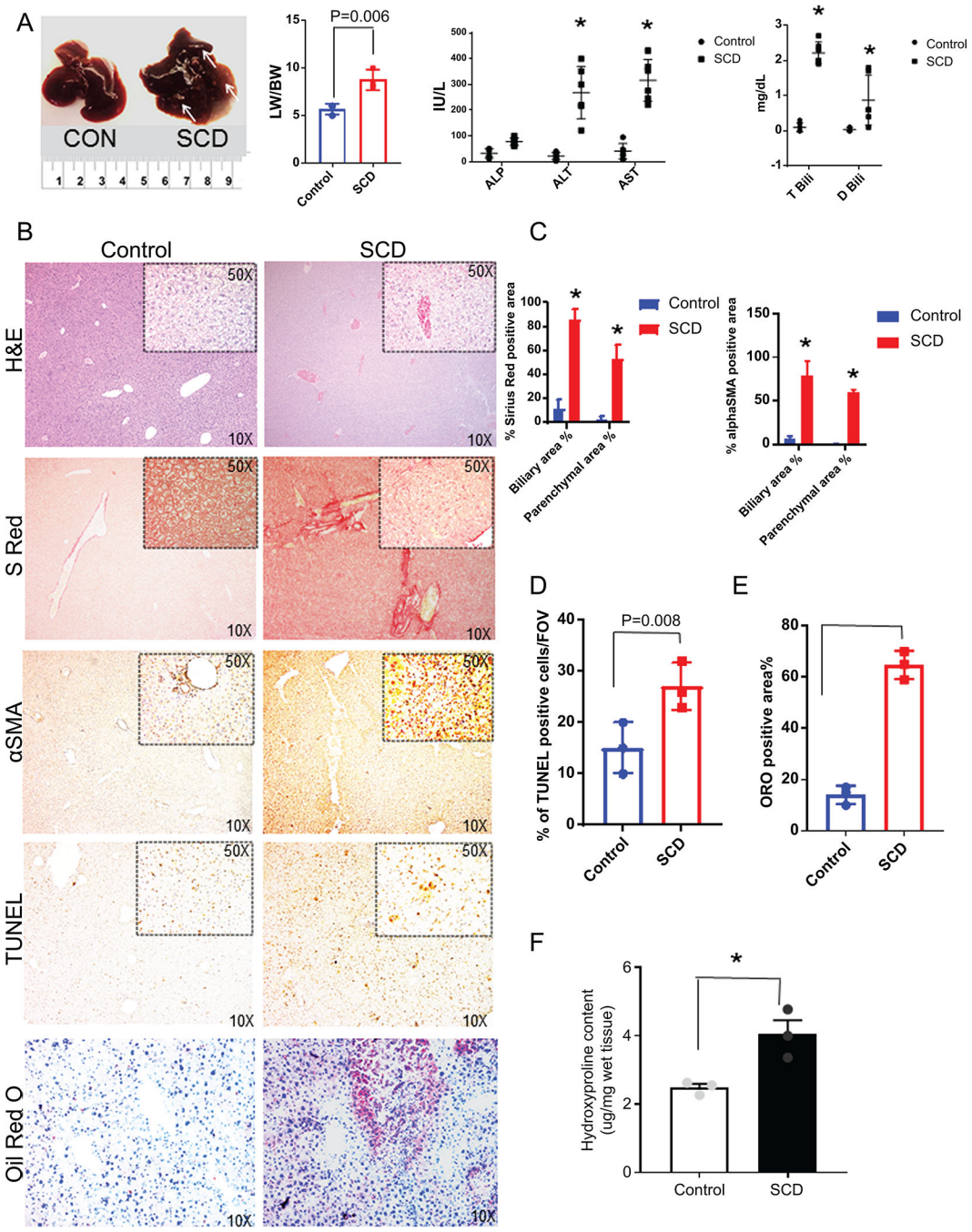

Figure 2: SCD mice have progressive liver injury and hyperbilirubinemia.

(A) Gross specimen of livers of control and SCD mice. SCD mice exhibit increased liver weight to body weight ratio. Serum biochemical analysis of liver enzymes ALT, AST and ALP in control and SCD mice. Serum analysis of direct and total bilirubin levels in control and SCD mice.**(B)** Immunohistochemical characterization of control and SCD mice. H&E, sirius red, αSMA, TUNEL and Oil-Red-O staining of control and SCD liver sections revealed increased injury, fibrosis, apoptosis inflammation and steatosis in SCD liver. **(C)** Quantification of biliary and parenchymal fibrosis as seen by Sirius red and αSMA positive

staining. **(D)** Quantification of TUNEL positive cells in control and SCD liver. **(E)** Quantification of Oil-Red-O staining in control and SCD liver. **(F)** Hydroxyproline content in the livers from control and SCD mice. * denotes $p<0.05$.

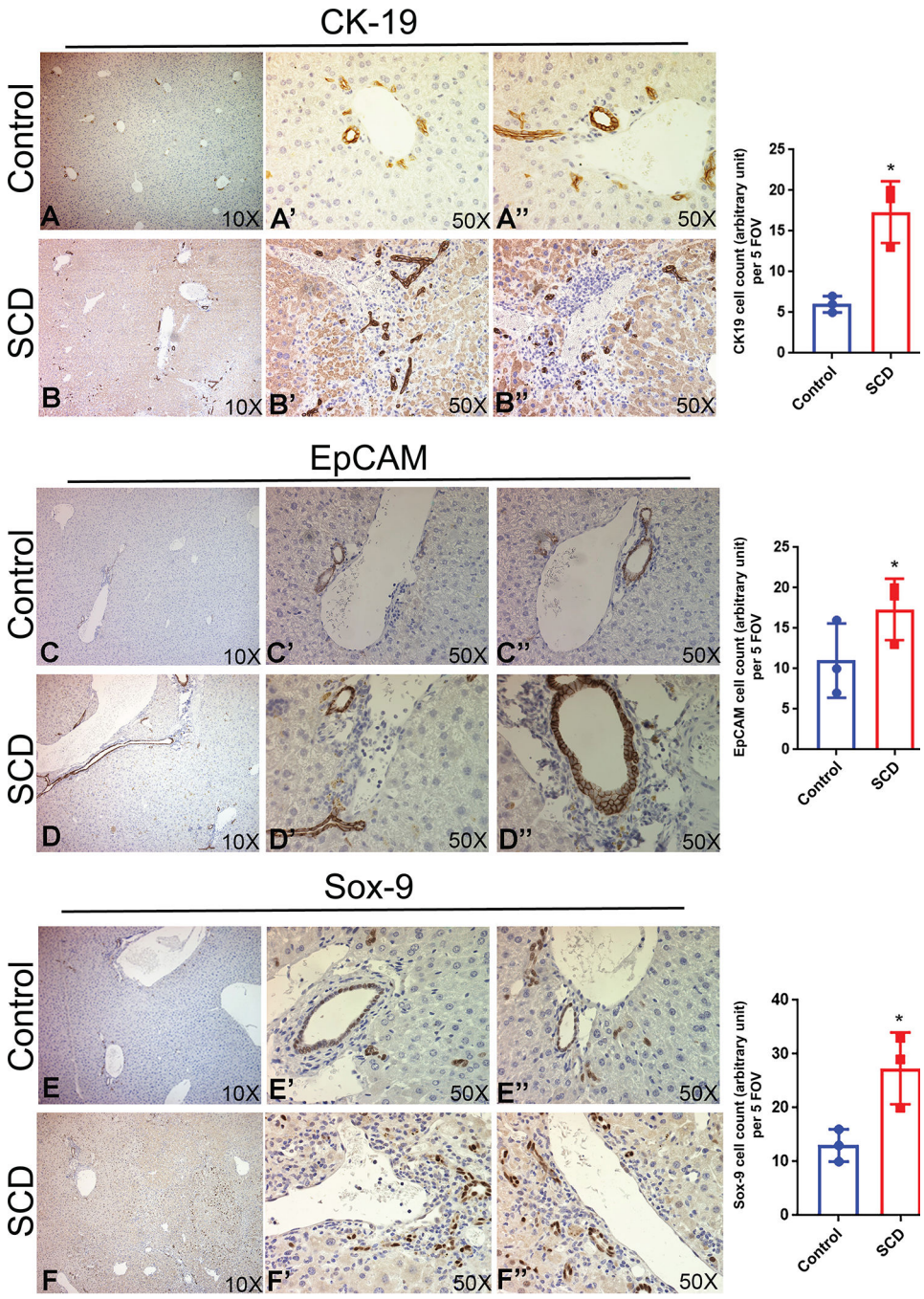

Figure 3: SCD liver exhibit an increase in ductular reaction.

IHC of cholangiocyte markers in control and SCD mouse liver. **(A-B)** SCD mouse liver showed an increase in the ductular reaction by CK19 positive staining compared to control liver. (**C-D**) The liver of SCD mice showed highly enriched EpCAM signal compared to control. (**E-F**) A prominent increase in Sox-9 staining was seen in the liver of SCD mice. Quantification of CK-19, EpCAM and Sox-9 positive ductular cells in control and SCD mouse liver tissue from 20 random fields. * denotes $p<0.05$.

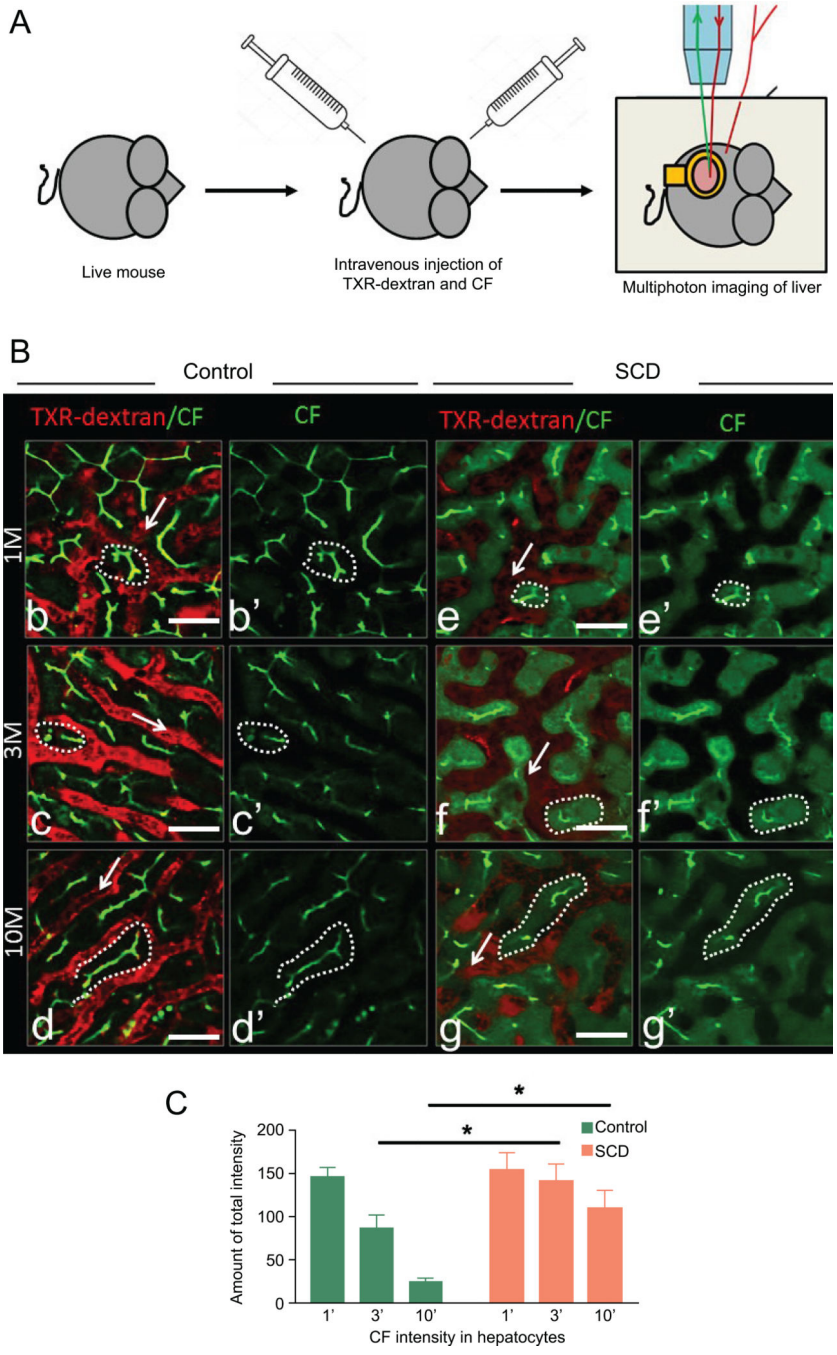

Figure 4: qLIM imaging reveals reduced bile flow in SCD liver.

(A) Schematic diagram of qLIM imaging of mice using CF and TXR-dextran. **(B)** *intravital* time series images of (**b-d'**) control and (**e-g')** SCD mice liver. 1**(b,e)**, 4**(c,f)** and 10 **(d,g)** minutes post administration of CF (green) and TXR-dextran (red). **(C)** Quantification of CF intensity in hepatocytes at 1', 4' and 10' after injection in control and SCD mouse liver. SCD liver showed a significant increase in CF intensity at 4' and 10' as compared to control liver. * denotes $p<0.05$. Scale bar 30 um.

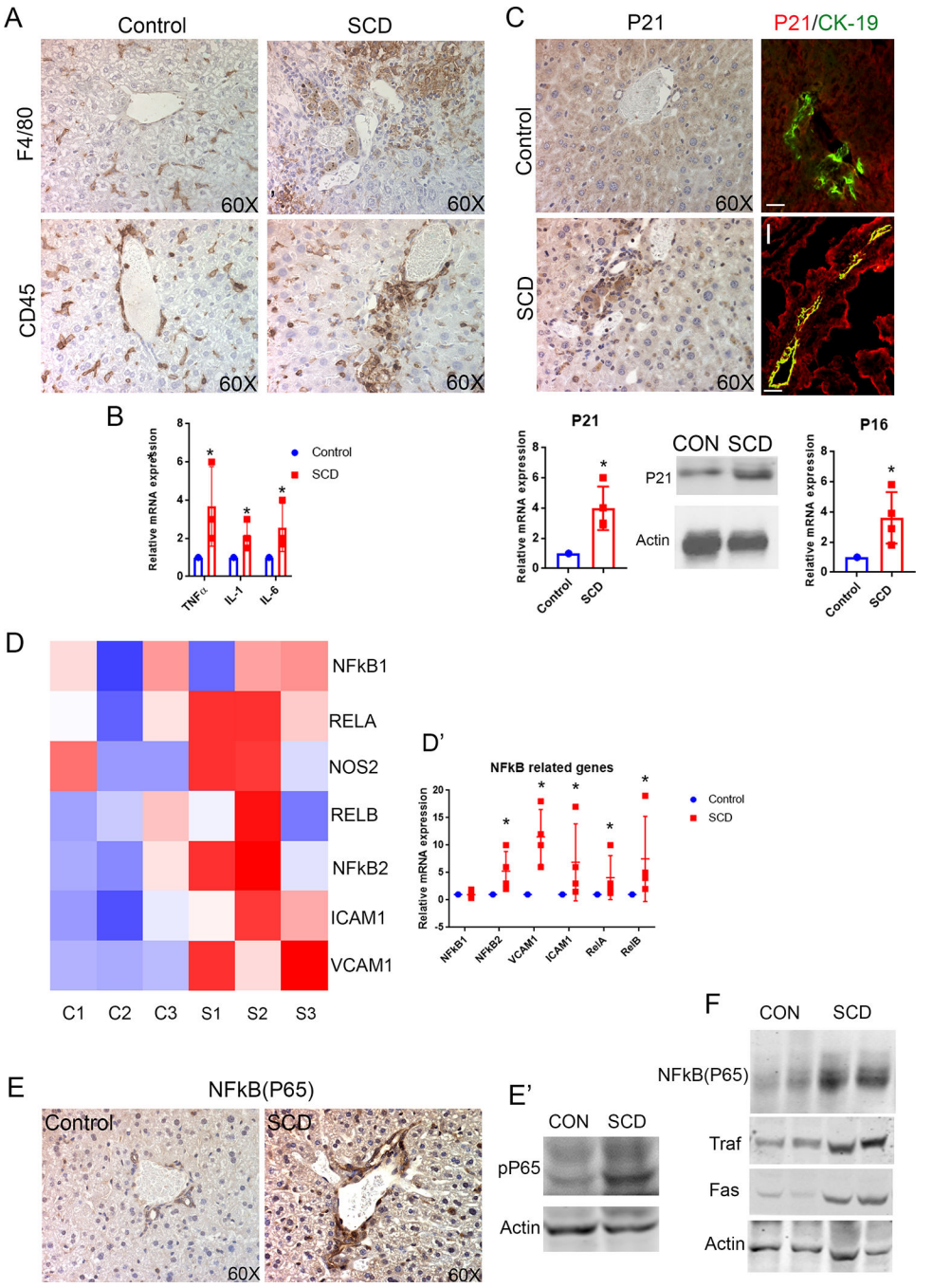

Figure 5: SCD is associated with increased cholangiocyte senescense and NF-kB activation in the liver.

(**A**) F4/80 and CD45 staining and quantification showed increased inflammation in SCD mouse liver. (**B**) qRT-PCR analysis of control and SCD mice liver exhibit an increase in mRNA expression of TNFα, IL-1, and IL-6. (**C**) IHC for P21 showed an increase in cholangiocyte positive P21 in SCD mouse liver. IF of P21/CK-19 exhibits almost complete colocalization of P21 (red) CK-19 (green) in SCD mouse liver. qRT-PCR analysis showed an increase in mRNA level of P21 in SCD mouse liver. Wetern blot showed increase in P21

expression in SCD liver. qRT-PCR analysis showed increase in mRNA level of P16 in the liver of SCD mice. (**D**) Heat maps consisting of selected genes involved in NF-kB pathway. (**D'**) Analysis of mRNA expression by qRT-PCR showed increase in mRNA expression of NFκB pathway components in SCD mice liver. (**E**) IHC for NFκB (P65) showed significantly increased expression in SCD cholangiocytes compared to control. Western Blot for phosphor-P65 confirms significant upregulation in the liver of SCD mice. (**F**) Western Blot for NF-kB(P65), Traf-1 and FAS exhibits increased expression in the liver of SCD mice. * denotes $p>0.05$.

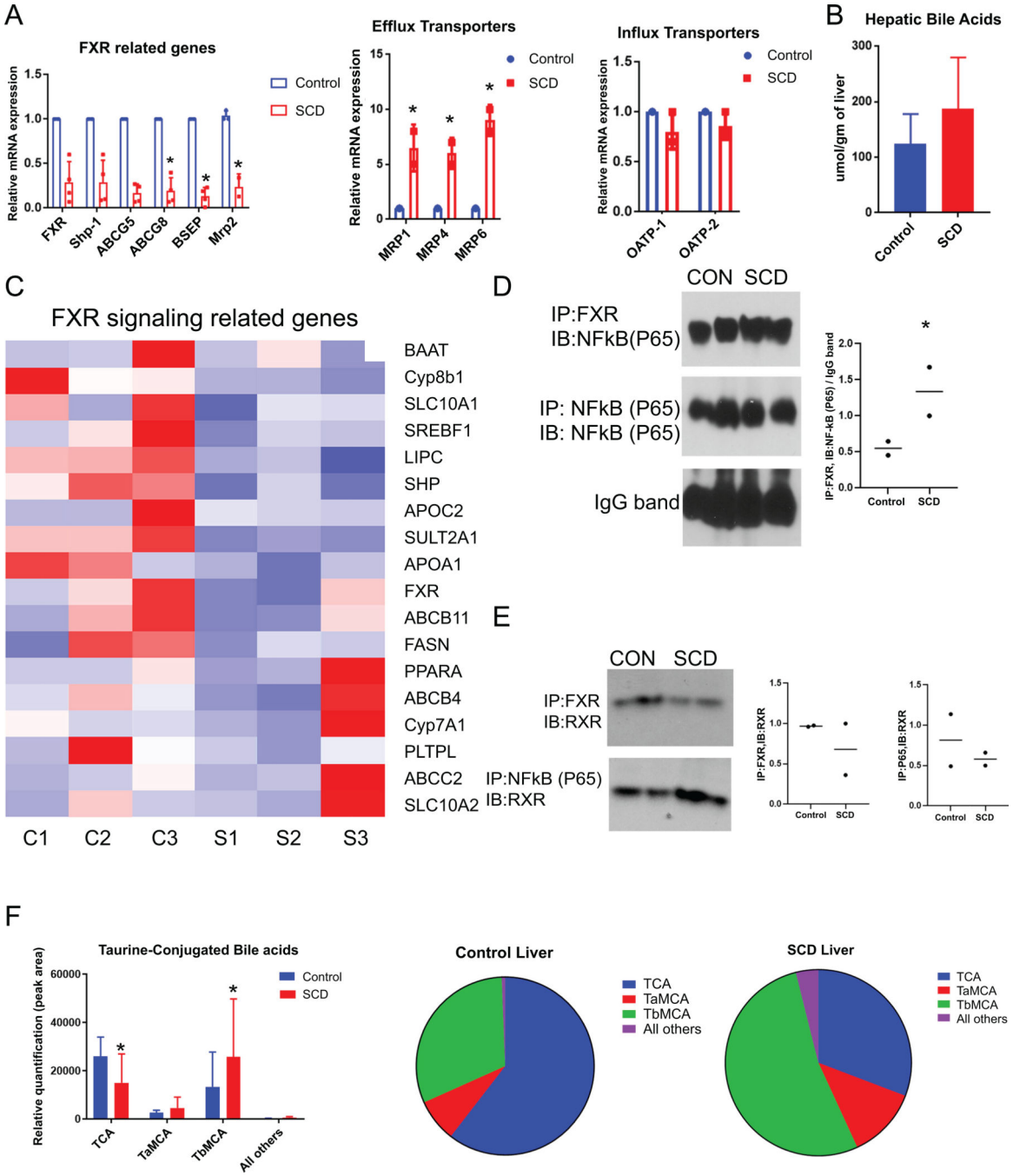

Figure 6: SCD mice exhibit impaired FXR signalling.

(**A**) qRT-PCR analysis reveals the expression level of FXR, Shp, BSEP, ABCG5, ABCG-8, and MRP2 in SCD and control mice liver. qRT-PCR analysis reveals the expression level of efflux and influx transporters in SCD and control mice liver. (**B**) Hepatic total bile acid is increased in SCD mice. (**C**) Heat maps consisting of selected genes involved in FXR pathway. (**D**) IP with FXR shows association with NF-kB in WT livers which was increased in SCD liver. Quantification of FXR and NF-kB(p65) binding. **(E)** IP shows FXR/RXR association is reduced in SCD as compared to control. Association between NF-kB and

RXR increased in SCD liver, as compared to control. Quantification of FXR and RXR binding. Quantification of RXR and NF-kB(P65) binding.(**F**) Analysis of bile acid species showed increase in TCA, TαMCA, and TβMCA in the livers of SCD mice, which resulted in a lower percentage of TCA in these livers when expressed qualitatively as a percentage of total bile acids (pie chart). * denotes $p>0.05$.

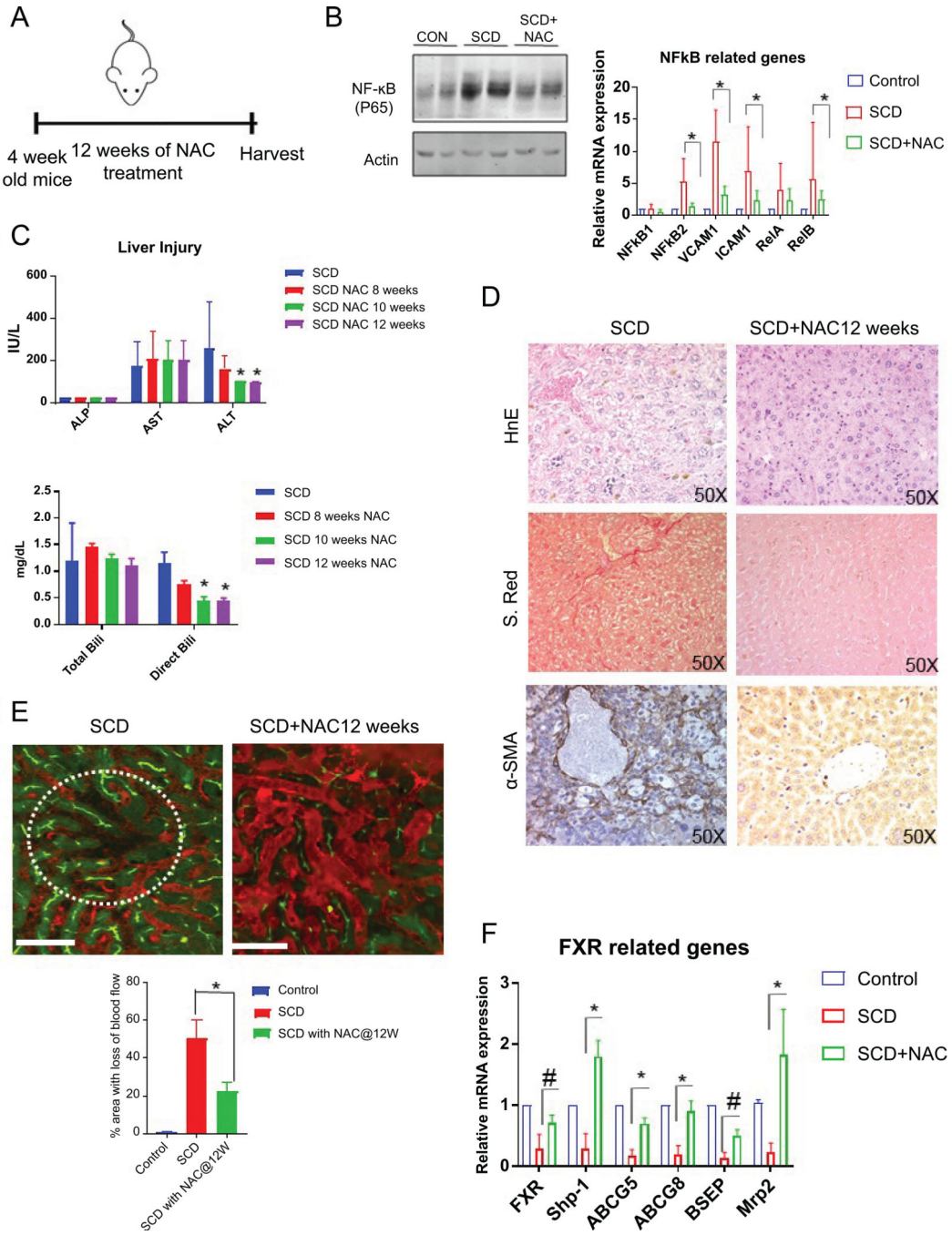

Figure 7: N-Acetyl-L-(+)-cysteine (NAC) can partially ameliorate liver injury in SCD mice.

(**A**) Schematic diagram of NAC administration scheme. (**B**) Western Blot for NF-κB(P65) confirms significant upregulation in the liver of SCD mice which was reduced upon NAC treatment. qRT-PCR analysis reveals the expression level of NF-κB and its target genes in control and SCD mice with or without NAC treatment. (**C**) Blood serum analysis showing ALP,ALT and AST level in control and SCD mice with or without NAC treatment after 4,8,10 and 12 weeks of treatment. Serum analysis of direct and total bilirubin levels in control and SCD mice with or without NAC treatment after 4,8,10 and 12 weeks of

treatment. **(D)** Immunohistochemical characterization of SCD mice with or without NAC treatment using H&E, sirius red and αSMA staining. (**E**) qLIM image of control and SCD liver. Dotted circle indicates the loss of flow of blood across the liver sinusoids in SCd liverwhich was ameliorated after NAC treatment. Quantification of the total area of liver with loss of blood flow in SCD and SCD+NAC mice. (**F**) qRT-PCR analysis reveals the expression level of FXR and its target genes in control, SCD and SCD mice with NAC treatment. * denotes $p>0.05$.# denotes $p>0.1$.

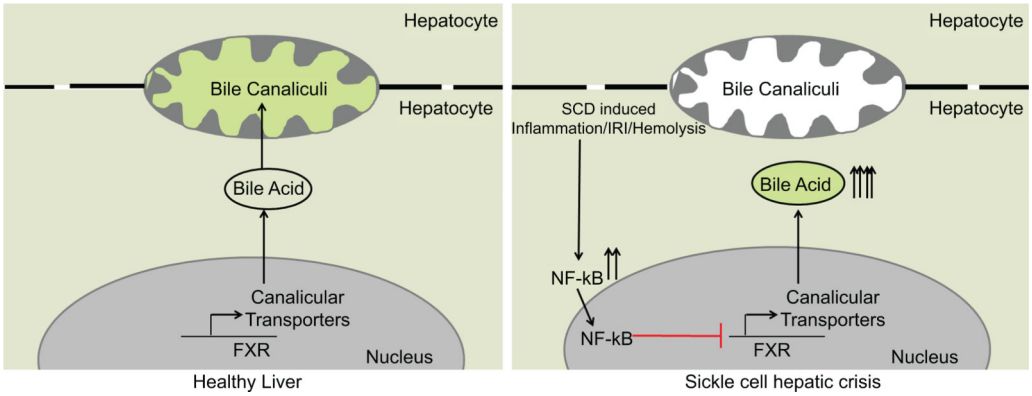

Figure 8: Impaired bile secretion promotes hepatobiliary injury in Sickle Cell Disease.

Schematic diagram depicting the mechanism of hepatobiliary injury in SCD. Sustained inflammation in SCD liver causes activation of NF-κB and its target genes which repressed FXR signaling in the liver of SCD mice leading to misexpression of canalicular bile transporters (BSEP, ABCG5,8 and MRP2), intrahepatic bile accumulation, and alered bile acid composition.